J Solid State Electrochem (1997) 1: 100–107

ORIGINAL PAPER

H. Cachet · R. Cortes · M. Froment · G. Maurin

Epitaxial electrodeposition of cadmium selenide thin films on indium phosphide single crystal

Received: 23 January 1992 / Accepted: 3 March 1997

Abstract Epitaxial CdSe layers were electrodeposited from a standard aqueous electrolyte onto a (111) InP single crystal. By using various characterization techniques (RHEED, XRD, HREM,...) it was demonstrated that a good epitaxy can be achieved by monitoring the experimental parameters very carefully, in particular the selenium concentration in the electrolyte and the deposition potential. For optimum conditions, the composition of the semiconducting layer is close to stoichiometry and the carrier density is around 1×10^{17} cm^{-3}.

Key words Epitaxial electrodeposition · Cadmium selenide · Indium phosphide

List of symbols

C_{Se}	Concentration of selenious acid in the electrolyte
V_B	Potential corresponding to the beginning of the diffusion plateau of the I/V curve [V]
i_L	Limiting current intensity of the plateau [A]
V_D	Deposition potential [V]
N	Charge carrier density [cm^{-3}]
C_p	Interfacial parallel capacitance [F.cm^{-2}]
Ω	Rotation speed of a rotating disk electrode [rpm]

Introduction

Thin films of various direct-band-gap semiconducting chalcogenide compounds, in particular cadmium chalcogenide compounds, are easily prepared by electrodeposition techniques from aqueous or organic solutions. By comparison with vapour phase deposition techniques, this low temperature and low cost method appears very attractive. After the pioneering works of Panicker et al. [1] numerous experimental or theoretical investigations were performed on CdX electrodeposition (where X represents Te, Se or S) or on some mixed compounds such as $CdTe_x\ Se_{1-x}$ or $Hg_xCd_{1-x}Se$ [2–4]. In most cases these layers are polycrystalline with a small grain size (typically 10–1000 nm). Their composition often differs from the correct stoichiometry, generally because of the presence of a slight excess of X atoms. The crystal quality as well as the composition of these materials are strongly dependent on the experimental preparation conditions (electrolyte composition, temperature, current intensity, potential,...) and in particular on the substrate properties. Finally, to get significant semiconducting properties it is necessary to apply thermal treatments to increase the grain size and improve the composition of the compound. In this way it has been possible to build large photovoltaic CdTe/CdS solar cells at a very low cost [5, 6]. For other applications such as optoelectronic devices the junction between the layer and the single crystal substrate (Si, GaAs, InP,...) has to be of excellent quality, characterized by an epitaxial relation between the two crystal lattices. It has been proved by Golan et al. that it is possible to obtain epitaxial growth of CdSe nanocrystals onto (111) gold films by electrodeposition from a non-aqueous electrolyte [7]. In the same way, Stickney et al. obtained epitaxial growth of CdTe [8] or CdSe [9] layers onto (100) or (111) gold faces by using the electrochemical atomic layer epitaxy (ECALE) technique, which consists in the alternate deposition of monolayers of the two components in separate solutions and under underpotential conditions. Recently, Lincot et al. [10] succeeded in electrodepositing a (111) CdTe layer in epitaxy with the $(\bar{1}\bar{1}\bar{1})$ face of an InP single crystal in spite of the large mismatch (10.5%) between CdTe and InP lattice parameters. However, the best results were obtained in the presence of a thin CdS film which was

H. Cachet (✉) · R. Cortes · M. Froment · G. Maurin
UPR 15 du CNRS "Physique des Liquides et Electrochimie",
Université Pierre et Marie Curie, 4 place Jussieu,
F-75 252 Paris Cedex 05, France
e-mail: gma@ccr.jussieu.fr

chemically deposited on the bare InP crystal before the CdTe electrodeposition from an acidic aqueous electrolyte. It was assumed that the CdS intermediate film increases the chemical bond and plays the role of a buffer layer which allows the matching between the two crystal lattices.

This paper presents results on the direct electrodeposition of CdSe thin films onto an n-type (111) single crystal of indium phosphide. It is shown that epitaxial growth can be obtained without the use of a CdS buffer layer owing to a more favourable lattice mismatch (3.6%) and precise control of the experimental conditions of the CdSe electrodeposition process.

The usual method for the electrodeposition of polycrystalline layers of CdSe from an aqueous solution is very similar to that for CdTe. In both cases, the electrolyte is a concentrated acidic solution of cadmium ions in which a small quantity of chalcogen precursor (chalcogen oxide or, for CdSe, selenious acid) is dissolved. When the potential applied to the working electrode is driven towards the more negative value (cathodic direction) three characteristic zones can be distinguished in the current intensity versus voltage response. In the first zone, chalcogen-rich layers grow, while in the third, metallic cadmium is deposited. The definite semiconducting compound, with the metastable cubic blende structure of the n-type, is obtained in the middle zone, that is to say in a potential range where pure cadmium would normally be dissolved. In an elemental model [11], the overall reaction was written as:

$$Cd^{++} + X^{IV+} + 6e^- \Rightarrow CdX \quad (1)$$

This reaction can be decomposed into three partial equations:

$$X^{IV+} + 4e^- \Rightarrow X^0 \quad (2)$$

In the presence of the X^0 species, cadmium ions can be reduced in underpotential conditions according to

$$Cd^{++}\ (X^0) + 2e^- \Rightarrow Cd^0\ (X^0) \quad (3)$$

giving finally the crystallized definite compound:

$$Cd^0 + X^0 \Rightarrow CdX \quad (4)$$

According to Kroger [12], the shift towards the less negative potential of the reduction of Cd^{++} ions in the presence of X^0 results in the gain of the Gibbs energy of formation of the definite compound. However, this mechanism can be disturbed, especially at a less negative potential, by the nucleation and growth of non-allied chalcogen [13]

$$X^0 \Rightarrow X_{crystal} \quad (5)$$

It has frequently been observed that the occurrence of this parasitic reaction is strongly dependent on the substrate nature and the cleanliness of the surface [14].

CdSe electrocrystallization differs from that of CdTe in some respects. For CdTe, the experimental domain is very narrow, due both to the very weak solubility of TeO_2 and to the restricted potential range where CdTe of good quality is obtained (a few tens of millivolts apart from the equilibrium potential of metallic cadmium). Conversely, for CdSe, the solubility of SeO_2 or $H_2Se_2O_3$ is much greater and the definite compound can be obtained in a potential range which can be greater than 200 mV. Loizos et al. [15] proved that the potential range where CdSe is effectively obtained corresponds precisely to the diffusion plateau of the polarization curve, where the current is totally limited by mass transport of $Se_2O_3^{--}$ ions. The limiting current intensity i_L, as well as the lateral extension of the plateau region, depend on $C_{Se,}$ the chalcogen precursor concentration (selenium oxide or selenious acid) in the bath. The same authors studied the quality of the semiconducting CdSe layers by using X-ray powder diffraction and by measuring their efficiency for light conversion in a photoelectrochemical cell. They observed that the best results are obtained at pH 2.2 ± 0.2 with a low C_{Se} value (typically 0.5×10^{-3} M) and for a deposition potential V_D corresponding to the beginning of the plateau region V_B.

Experimental

In most experiments, the substrate was made of InP single crystals supplied by Applications Couches Minces (France). They were cut along the (111) plane with both the (111) and $(\bar{1}\bar{1}\bar{1})$ faces chemomechanically polished by the supplier. The InP single crystals were n type sulfur doped and the carrier concentration was 2.5×10^{18} cm^{-3}. The working area was typically 1 cm^2. A back ohmic contact was obtained by a liquid Ga-In dot. Prior to deposition, the surface was rinsed in methanol, etched with a bromine methanol mixture (1% by volume) for 30 s and then dipped in sulfuric acid (3 M) for 5 min in order to remove the surface oxide layer. Finally, the InP substrates were thoroughly rinsed in deionized water before being introduced into the electrolytic cell.

In order to determine the experimental conditions leading to "good" CdSe electrodeposits, preliminary experiments were carried out using as substrate a rotating disc electrode made of polycrystalline titanium. Prior to the deposition, the titanium electrodes were mechanically polished with 0.3 μm alumina powder and immersed for 5 min in 3 M sulfuric acid to remove the native oxide film.

Cadmium selenide was cathodically deposited in a three-electrode cell from an acid solution containing 0.2 M $CdSO_4$ to which various amounts of selenious acid ($0.125 \times 10^{-3} \leq C_{Se} \leq 5 \times 10^{-3}$ M) were added. The pH was adjusted to 2.2 ± 0.05 and the temperature maintained at 80 ± 0.5°C. The mass transport was controlled using either a rotating disc electrode in the preliminary experiments or by maintaining the InP substrate vertically in a fixed position and stirring the electrolyte with a magnetic barrel at a constant rotation rate. The working electrode potential, measured against a saturated mercurous sulfate electrode (SSE), was monitored by a potentiostat. A large platinum grid was used as counter electrode.

The characterization of the CdSe electrodeposits was achieved by using various techniques. The thickness and the composition of the electrodeposited films were evaluated by Rutherford back scattering (RBS) measurements. Scanning electron microscopy (SEM) was used to observe their surface morphology. Reflection high energy electron diffraction (RHEED) gave a preliminary indication of the crystal quality of the layer and its orientation with respect to the substrate. A quantitative determination of the

structure and the epitaxial orientation of the films was achieved by an X-Ray diffraction (XRD) method, using a five-circle goniometer specially designed for thin-film studies [16]. In this device the incident beam is at a glancing angle (ca. 0.6°), and the X-Ray detector is positioned at a 2θ angle corresponding to a Bragg diffraction angle characteristic either of the substrate or of the deposit material. The sample is rotated around its symmetry axis. The intensity of the diffracted beam versus the rotation angle gives information on the relative orientation of the layer and the quality of the epitaxial fit. CdSe/InP samples were cross-sectioned and thinned by ion milling for high resolution electron microscopy (HREM) observations, allowing structural characterization of the interface at the atomic level. The carrier concentration N was estimated by measuring the capacitance of a liquid junction as a function of the applied potential. The electrolyte was a 0.5 M $LiClO_4$ solution in an acetate buffer at pH 4.6. Electrochemical a.c. impedance measurements were carried out in a three-electrode cell configuration under potentiostatic control, using a TF2000 Voltech frequency response analyser. The parallel capacitance C_P, deduced from impedance measurements in the 10 Hz–100 kHz frequency range, was generally found to be independent of the frequency above 50 kHz. Hence C_P^{-2} versus potential Mott-Schottky plots were recorded at 95 kHz every 50 mV from the flat band potential (ca. −1.15 V/SSE) to +0.05 V/SSE.

Results

Preliminary investigations

In order to determine precisely the limits of the experimental domain of CdSe electrodeposition, polarization curves were drawn using a rotating titanium disc electrode for various rotation rates and various C_{Se} values. Figure 1 represents a set of stationary polarization curves obtained for a constant rotation rate Ω = 500 rpm and for different C_{Se} values. The dashed line is relative to the pure metallic cadmium deposition (C_{Se} = 0). It can be seen that the lateral extension of the central plateau region, which results from the growth rate limitation by the diffusion of selenious ions in the liquid phase, is reduced as the selenium oxide concentration is increased. An increase in the rotation rate would have a similar effect. As a consequence, the potential V_B, which, according to Loizos et al. [15], corresponds to the best CdSe deposits, is strongly dependent on C_{Se} and on the hydrodynamic conditions. For example, for Ω = 500 rpm, according to Fig. 1, V_B equals −0.940 ± 0.015 V for $C_{Se} = 0.5 \times 10^{-3}$ M, whereas it is shifted to −1.14 V when C_{Se} is increased to 4×10^{-3} M. For $C_{Se} \geq 5 \times 10^{-3}$ M, the diffusion plateau is reduced to zero, and it is no longer possible to obtain the CdSe definite compound. The first part of the I/V curve (drawn as a dotted line) is not stationary because of the formation of elemental selenium outgrowths.

A limited number of polarization curves were also performed using a stationary InP single-crystal substrate. By comparing the limiting current densities i_L obtained with the two kinds of electrodes, it can be concluded that the hydrodynamic conditions ensured by the mechanical stirring near the InP surface are similar to those for the disc electrode rotating at ca. 150 rpm. From this comparison, it was possible to pre-determine the limits of the plateau region for InP stationary samples as a function of C_{Se}.

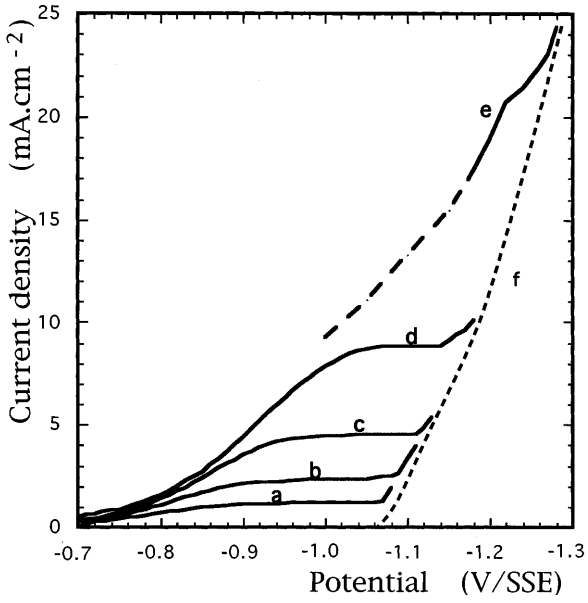

Fig. 1a–f Effect of the selenious acid concentration on the polarization curves obtained with a titanium rotating disc (∅ 1.2 cm, 500 rpm) electrode immersed in an electrolyte containing 0.2 M $CdSO_4$, pH 2.2, T 80°C. **a** C_{Se} 0.25×10^{-3} M, **b** C_{Se} 0.5×10^{-3} M, **c** C_{Se} 1×10^{-3} M, **d** C_{Se} 2×10^{-3} M, **e** C_{Se} 5×10^{-3} M, **f** C_{Se} 0 (metallic cadmium electrodeposition)

CdSe epitaxial growth

CdSe layers with a thickness of 30–250 nm, were electrodeposited either on the (111) or the $(\bar{1}\bar{1}\bar{1})$ face of an InP single crystal for various selenious acid concentrations ($0.25 \times 10^{-3} \leq C_{Se} \leq 5 \times 10^{-3}$ M) and for various potentials, inside or outside the plateau region. As for polycrystalline CdSe electrodeposits, epitaxial CdSe films always present the cubic blende structure. A systematic RHEED study reveals that the epitaxial growth of CdSe on InP strongly depends on the experimental parameters. Figure 2 shows RHEED patterns corresponding to the best conditions of epitaxy ($C_{Se} = 0.5 \times 10^{-3}$ M and $V_D = V_B = -0.95$ V/SSE). The RHEED pattern of Fig. 2b, which was obtained under the $\langle 1\ \bar{1}\ 0 \rangle$ azimuth, presents additional spots characteristic of the presence of an important density of twins parallel to the substrate surface. In these conditions, the epitaxial growth remains excellent at least up to 100 nm and does not depend on the nature of the InP face, either (111) or $(\bar{1}\bar{1}\bar{1})$.

For the same C_{Se}, but when V_D is driven away from V_B, RHEED patterns (Fig. 3) reveal an important deterioration of the epitaxial growth, characterized both by an attenuation of the single crystal diffraction spots and by the appearance of new diffraction rings. At V_D = −1.05 V/SSE (end of the plateau) (Fig. 3a), these

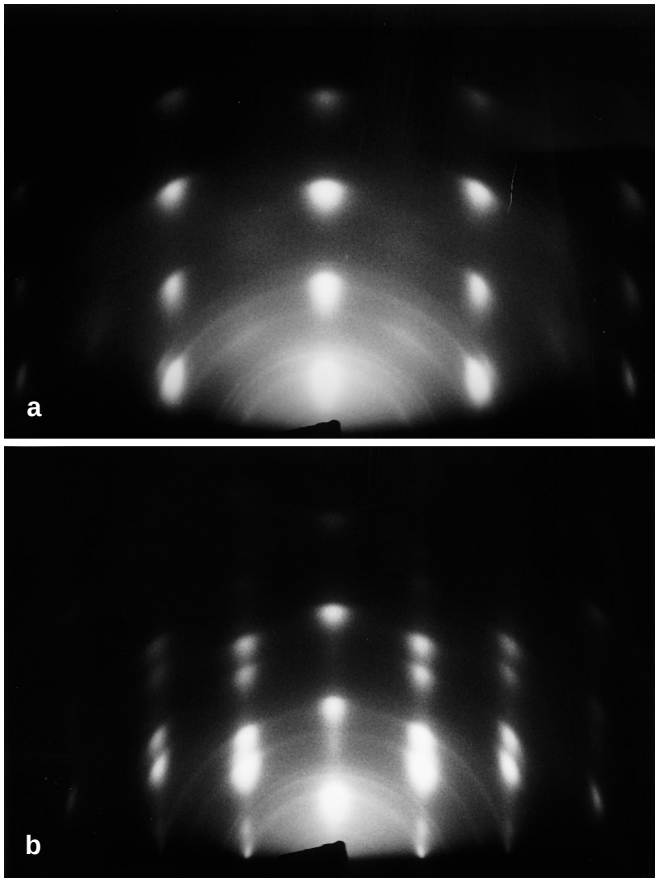

Fig. 2a,b RHEED patterns corresponding to the best epitaxial conditions of CdSe deposited on a $(\bar{1}\bar{1}\bar{1})$ InP face: C_{Se} 0.5×10^{-3} M, V_D −0.95 V/SSE, thickness 85 nm. **a** Observation under the $\langle 112 \rangle$ azimuth; **b** observation under the $\langle 1\bar{1}0 \rangle$ azimuth

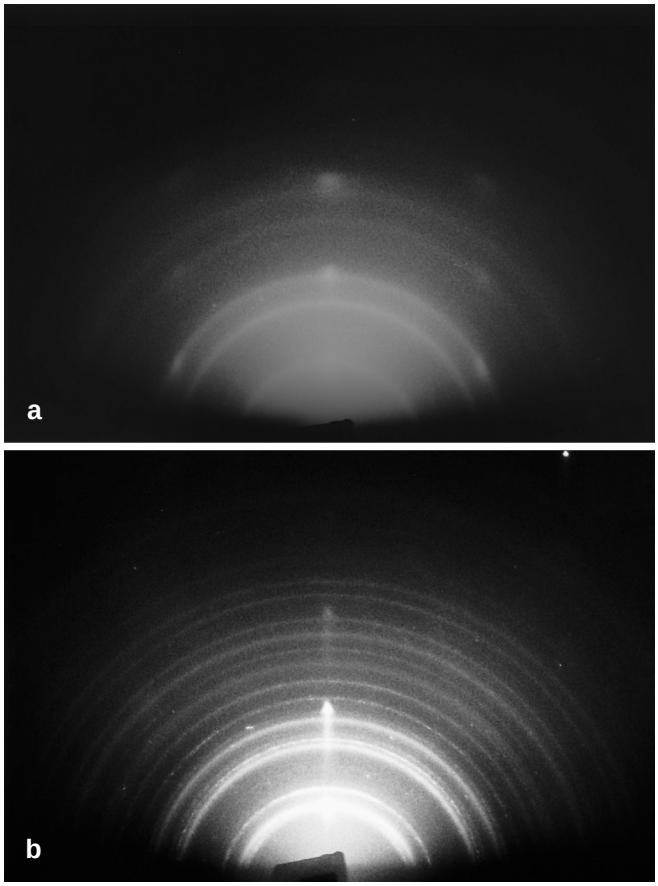

Fig. 3a,b RHEED patterns showing the deterioration of the CdSe epitaxial growth at potentials differing from V_B. **a** C_{Se} 0.5×10^{-3} M, V_D −0.85 V/SSE, thickness 32 nm; **b** C_{Se} 0.5×10^{-3} M, V_D −1.05 V/SSE, thickness 40 nm

rings correspond to a polycrystalline CdSe phase, whereas the RHEED patterns obtained in the potential region preceding the plateau (Fig. 3b) exhibit diffraction rings belonging mostly to polycrystalline red selenium. Accordingly, the SEM image of this last deposit (Fig. 4a) differs from that of an epitaxial deposit obtained in the best conditions (Fig. 4b). In particular, the white local irregularities correspond to the presence of elemental selenium. As illustrated by the RHEED pattern of Fig. 5, a loss of epitaxy is also observed when C_{Se} is slightly driven away from the optimum value, even if in each case V_D equals V_B. These results are confirmed by the RBS measurements. For a deposition potential preceding the plateau region, a strong excess of selenium is detected. The [Se]/[Cd] ratio is close to one at the beginning of the plateau, whereas this ratio tends to decrease slightly, reaching ca. 0.9 for more negative deposition potentials.

XRD diagrams obtained with the five-circle goniometer bring additional information on the CdSe/InP epitaxy. Figures 6a,b correspond to scans, with a 0.6° glancing angle, respectively, obtained with CdSe layers electrodeposited at −1.05 V/SSE, with $C_{Se} = 1 \times 10^{-3}$ M (Fig. 6a), and at −0.95 V/SSE with $C_{Se} = 0.5 \times 10^{-3}$ M (Fig. 6b). In Fig. 6a, the (220) CdSe diffraction peaks present a full width at half maximum (FWHM) of 10°, whereas, for the best conditions of epitaxy identified by RHEED observations (Fig. 6b), the FWHM of the CdSe peaks is only 4°. This value can be compared to the FWHM measured on the (220) peak of the InP substrate, obtained with a 6° glancing angle, which equals 0.25°. It is interesting to note that the FWHM found for the best conditions of electrodeposition is significantly smaller than that previously measured with CdSe films prepared by the chemical bath deposition technique onto (111) InP single crystals [17].

Another interesting feature can be seen in Fig. 6a,b: six peaks, corresponding to the (220) reflections of the CdSe cubic structure, are observed instead of three, as normally expected. This phenomenon indicates the presence of twinning in the CdSe layer parallel to the substrate surface, provided by the possibility for the (111) CdSe nuclei to grow in epitaxy with an InP or CdSe (111) face in two equivalent positions, with a 180° rotation between them [18]. The diffraction peak intensities are of the same order of magnitude for the two equivalent positions. Further analysis of the XRD patterns of Fig. 6 shows that the crystallographic directions

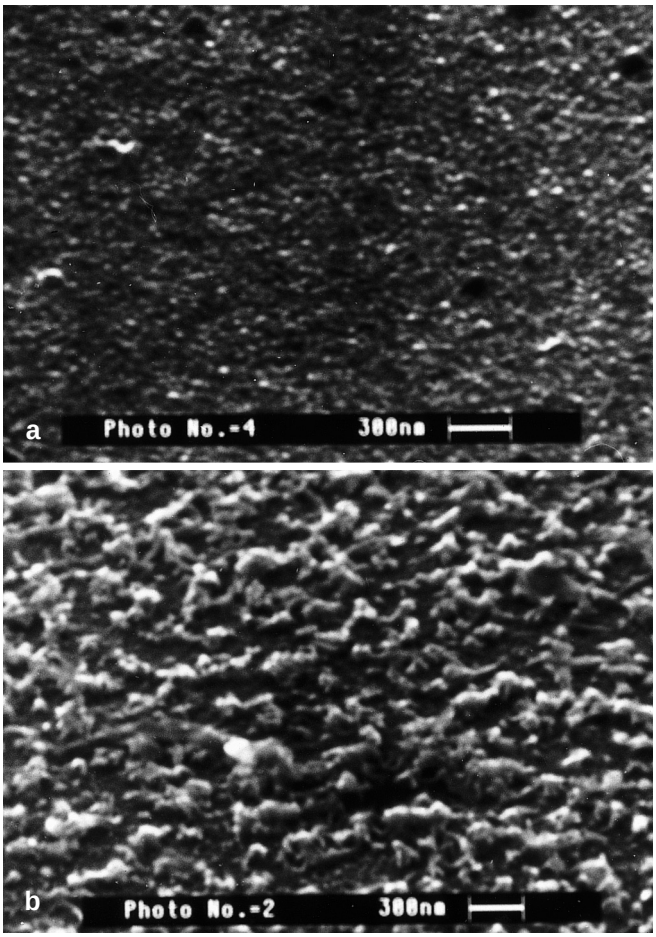

Fig. 4a,b SEM observations of the morphology of CdSe layers deposited on $(\bar{1}\bar{1}\bar{1})$. **a** C_{Se} 0.5×10^{-3} M, V_D −0.85 V/SSE; **b** C_{Se} 0.5×10^{-3} M, V_D −0.95 V/SSE

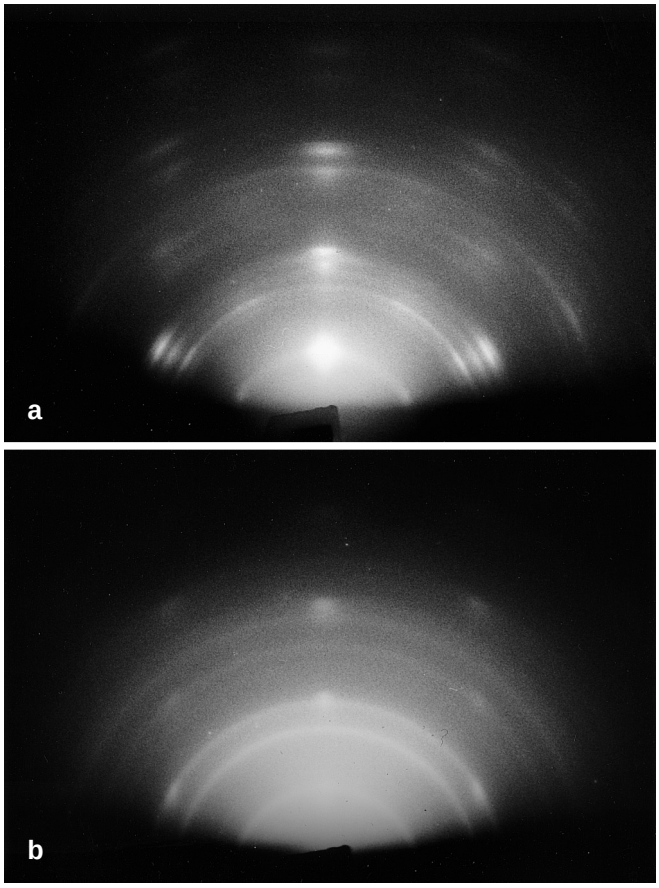

Fig. 5a,b RHEED patterns showing the influence of the selenious acid concentration on the CdSe epitaxial growth. **a** C_{Se} 0.25×10^{-3} M, V_D −0.95 V/SSE, thickness 40 nm; **b** C_{Se} 1×10^{-3} M, V_D −1.05 V/SSE, thickness 48 nm

of the epilayers are aligned with that of the InP substrate within 1.5°, whereas there is no rotation in the plane.

TEM images of CdSe/InP cross sections were obtained with the $\langle 1\bar{1}0 \rangle$ InP axis aligned along the incident beam direction. Figure 7a shows an abrupt interface and the presence of planar defects (twin planes or stacking fault) parallel to the interface. These observations confirm the results obtained by XRD. Another group of {111} twins planes are tilted at 71°. They are generated by the coalescence between domains in opposite epitaxial position. The high resolution image (Fig. 7b) reveals a low density of defects along the interface, proving an excellent epitaxy in spite of a 3.6% lattice mismatch between InP and CdSe.

Carrier density of CdSe layers

Figure 8 represents the Mott-Schottky plots obtained in the dark for CdSe layers electrodeposited on a titanium substrate at various deposition potentials V_D within the plateau region. C_{Se} was fixed at 0.5×10^{-3} M. These Mott-Schottky plots are never

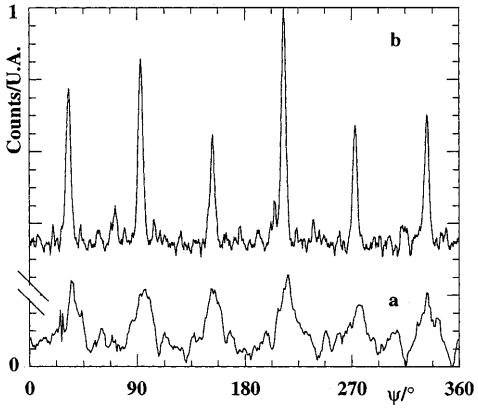

Fig. 6a–b XRD patterns of CdSe films deposited on InP $(\bar{1}\bar{1}\bar{1})$. The scans were obtained around an axis normal to the sample surface; influence of the growth conditions on the epitaxial growth. **a** Angle of incidence 0.6°, C_{Se} 1×10^{-3} M, V_D −1.05 V/SSE, thickness 60 nm, FWHM of the (220) CdSe reflections 10°; **b** angle of incidence 0.6°, C_{Se} 0.5×10^{-3} M, V_D −0.95 V/SSE, thickness 170 nm, FWHM of the (220) CdSe reflections 4°

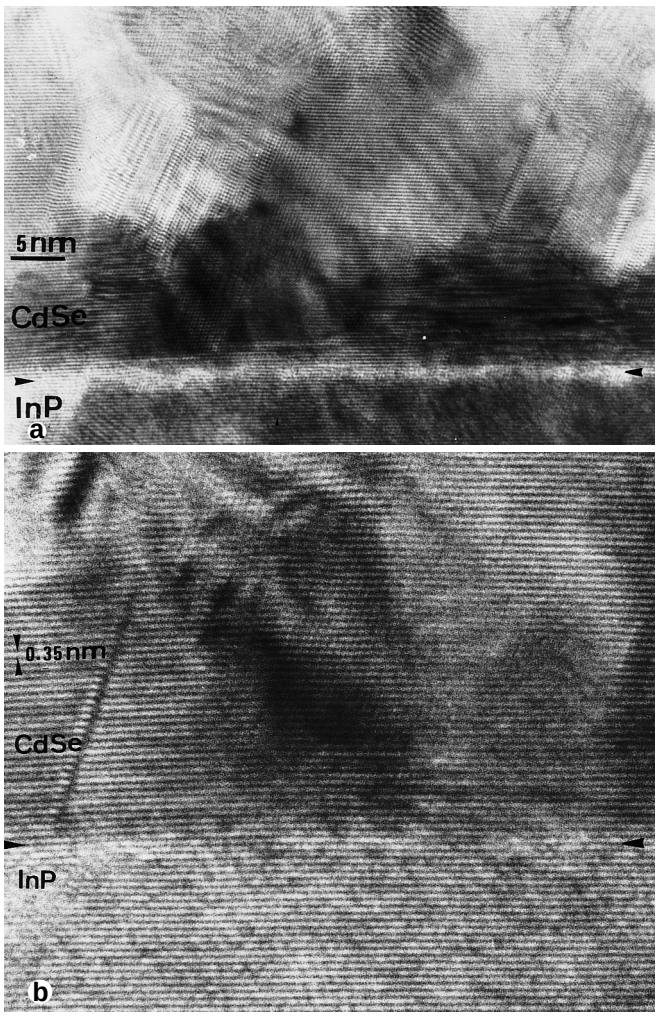

Fig. 7a,b TEM observation of a cross section prepared from an epitaxial CdSe film deposited on a $(\bar{1}\bar{1}\bar{1})$ InP face: C_{Se} 0.5×10^{-3} M, V_D −0.95 V/SSE. **a** Low magnification image showing the presence of planar defects in the CdSe film; **b** HREM image with (111) lattice planes; the *arrows* indicate the interface between InP and CdSe

totally linear, as expected for an ideal semiconductor. A linear region is observed only at low potentials, the slope of which can be used to estimate the charge carrier density N. A strong effect of V_D on the slope can be observed. The largest slope and the largest linear domain (over 0.50–0.60 V) are simultaneously obtained for $V_D = -0.925$ V/SSE, that is to say the potential which corresponds precisely to the best CdSe epitaxial growth onto InP (see Fig. 2, 5 and 6). It is interesting to note on the Mott-Schottky plots that the slope change occurs for a space charge layer width of ~100 nm as deduced from the value of the capacitance at the "break" point. This value is much lower than the actual thickness (250 nm) of the CdSe layers as determined by RBS analysis. The curvature of the Mott-Schottky plots may rather be attributed to the presence of bulk electronic states, the density of which would be at a minimum for $V_D = -0.925$ V/SSE. Figure 9 shows the variations of N against V_D. For deposition potentials corresponding to the beginning of the current plateau (−0.950 to −0.875 V/SSE depending on C_{Se}, Fig. 1), N is close to 1×10^{17} cm^{-3}. N tends to increase for more negative potentials when V_D approaches the cadmium deposition potential.

Mott-Schottky plots were also performed with a (111) InP single crystal (Fig. 10, curve a) and with CdSe/InP epitaxial layers electrodeposited in the optimum conditions (Fig. 10, curve b). The Mott-Schottky plot relative to the InP single crystal is perfectly linear and corresponds to a carrier concentration $N = 1.0 \times 10^{18}$ cm^{-3}, in close agreement with the specifications of the supplier. Furthermore, there is no frequency dispersion within the 10 Hz–100 kHz frequency range. In the case of the CdSe/InP system, a more complicated curve is observed resembling those obtained with the CdSe/titanium system (Fig. 8). Hysteresis effects appear when comparing the direct and the reverse potential scans. The capacitance-voltage curve

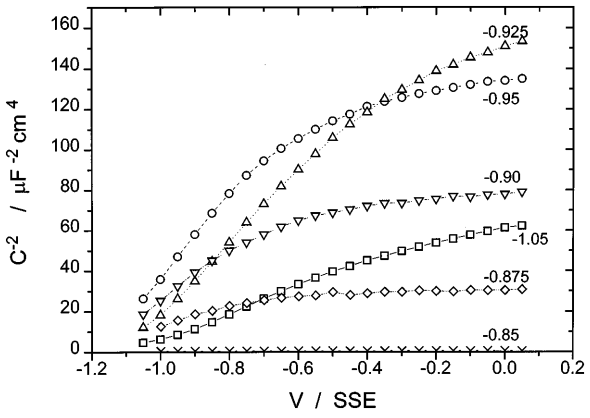

Fig. 8 Mott-Schottky plots of CdSe layers electrodeposited on titanium substrates in contact with 0.5 M $LiClO_4$ in acetate buffer at pH 4.6, for various deposition potentials along the current plateau; C_{Se} 0.5×10^{-3} M

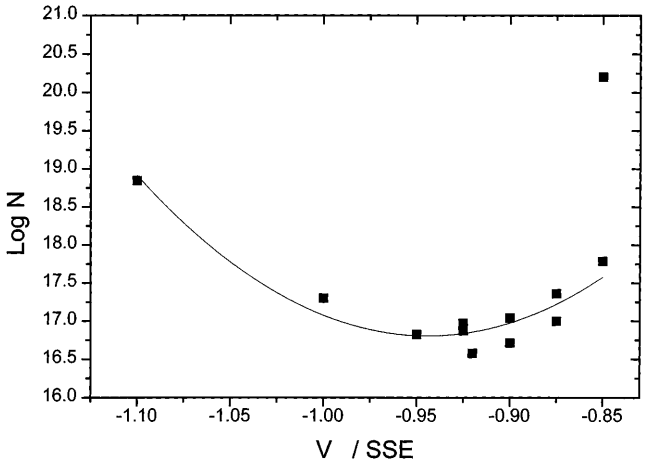

Fig. 9 Variations of the carrier concentration N of CdSe layers against the deposition potential; C_{Se} 0.5×10^{-3} M. The *full line* is a parabolic approximation of the data without physical meaning

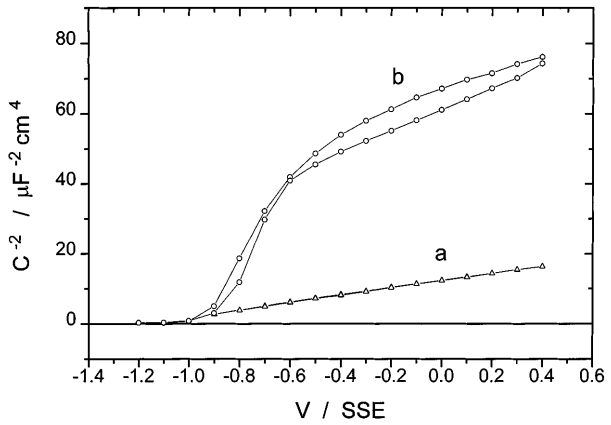

Fig. 10 Mott-Schottky plots obtained with a 0.5 M $LiClO_4$ solution in acetate buffer at pH 4.6, **a** with a (111) InP single crystal, and **b** with an electrodeposited CdSe layer epitaxially deposited onto InP (C_{Se} 0.5×10^{-3} M, V_D −0.93 V/SSE)

corresponds to an (n)InP/(n)CdSe structure, i.e. an n–n isotype heterojunction. The conduction band discontinuity is not larger than 0.4 eV, leading to equilibrium conditions close to a flat-band situation. The analysis of the capacitance response versus potential is not straightforward, since the applied potential is, in principle, distributed throughout the structure [20]. Taking the data of Fig. 8 into consideration, the carrier density of the CdSe layer may be ten times smaller than that of the highly doped InP substrate. In such a situation, it is reasonable to assume that any voltage change mainly occurs over the less doped side of the junction, i.e. over the CdSe layer. It means that the structure would practically behave as a simple metal-semiconductor junction, with a depletion regime only established in the CdSe side of the junction. Within this simplified picture, a carrier density of 1×10^{17} cm^{-3} can be estimated from the slope in the −0.9 to −0.6 V/SSE potential range and 4×10^{17} cm^{-3} from the mean slope at more positive potentials. The break in the Mott-Schottky diagram cannot be attributed to the space charge width reaching the geometrical thickness of the CdSe overlayer. Most probably, it arises from the presence of bulk states, as for the data of Fig. 8. The InP capacitance response is not observable, suggesting that the InP substrate would be held near flat-band conditions.

Conclusion

According to our knowledge, for the first time, thin films of a II-VI semiconductor have been epitaxially electrodeposited on a III-V single crystal from an aqueous electrolyte, without buffer layer. This result proves that the electrodeposition technique is a simple and interesting method to prepare heterojunctions without vacuum technology or heat treatment.

The whole set of methods used for characterizing the electrodeposited CdSe epilayers gives evidence that the experimental conditions have to be monitored very carefully. In particular, the precursor concentration C_{Se} has to be small enough and the deposition potential has to be maintained at a value which corresponds to the beginning of the current plateau resulting from the control of the process by mass transport of the selenium precursor. These optimum conditions are completely identical to those previously identified for the strongly textured growth of polycrystalline CdSe deposits onto various inactive substrates such as titanium, nickel or tin oxide conducting glass.

In both cases, it appears that there is a strong correlation between the thin film composition and the growth process. When the optimum conditions are fulfilled, the overall Cd/Se ratio is close to one, the charge carrier concentration is minimal and the potential range where the Mott-Schottky plot is linear is the largest, indicating that the gap state distribution is repelled deeper into the band gap. These conditions are favourable for the achievement of the alternate nucleation of 2D monolayers of Se and Cd according to Eqs. 2 and 3, followed by a 2D layer-by-layer growth. By means of a transient analysis technique, Sugimoto and Peter [19] studied the nucleation of CdTe onto three different surface orientations of an Si single crystal. Whereas, in this case, there is no evidence of epitaxial growth, current transients were characteristic of a 2D nucleation. At each stage of the 2D layer-by-layer process there is a certain probability that the new nuclei introduce errors in the stacking order of the dense planes, giving rise to twinning or to stacking faults as observed by RHEED, XRD or in the cross-section TEM images. These crystal defects have a low energy and can be considered as a transition between the cubic blende structure and the hexagonal wurtzite structure. In the cubic blende structure, the Se or Cd monolayers are parallel to (111) planes. For polycrystalline deposits, this leads to a strong $\langle 111 \rangle$ preferred orientation. When an InP single crystal is used as substrate, it is very probable that the In-rich (111) or the P-rich $(\bar{1}\bar{1}\bar{1})$ faces will be favourable to the 2D nucleation of CdSe.

As soon as the experimental conditions depart from the optimum, the deviation from stoichiometry appears to be detrimental to the 2D nucleation/growth process both for polycrystalline and epitaxial layers and tends to favour a 3D nucleation of small grains. For a deposition potential more negative than V_B, most of the cadmium atoms in excess are more probably located in the grain boundaries, whereas the core of the grains is made of stoichiometric CdSe with a slight increase in the charge carrier concentration. For a deposition potential preceding the plateau region, the interfacial concentration of selenious ions is no longer zero, allowing the dendritic growth of elemental selenium and giving rise to heterogeneous and porous layers.

References

1. Panicker MPR, Knaster M, Kroger FA (1978) J Electrochem Soc 125:566
2. Rauh RD (1988) In: Finklea (ed) Studies in physical and theoretical chemistry, vol 55. Elsevier, Oxford, pp 277–328
3. Gruszecki T, Holmström B (1993) Solar Energy Materials and Solar Cells 31:227.
4. Rajeshwar K (1992) Adv Mater 4:23
5. McGregor SM, Dharmasada IM, Wadsworth I, Care CM (1996) Opt Mat 6:75
6. Ozsan ME, Johnson DR, Sadeghi M, Sivapathasundaram D, Lincot D, Mokili B, Froment M, Vedel J (1995) In: Freiesleben W, Palz W (eds) Proceedings of the 13th European Photovoltaic solar energy conference, Nice (France) vol II, Stephens & Associates, pp 2115–2118
7. Golan Y, Margulis L, Hodes G, Rubinstein I, Hutchinson JL (1994) Surf Sci 311:L.633
8. Suggs DW, Stickney JL (1993) Surf Sci 290:375
9. Lister TE, Huang BE, Stickney JL (1995) Comm. Meeting of the Electrochem. Soc. (Chicago). Abstract no. 890
10. Lincot D, Kampmann A, Mokilii B, Vedel J, Cortes R, Froment M (1995) Appl Phys Lett 67:2355
11. Loizos Z, Spyrellis N, Maurin G, Pottier D (1989) J Electroanal Chem 269:399
12. Kroger FA (1982) J Electrochem Soc 125:2028
13. Tomkiewicz MT, Ling I, Parsons WS (1982) J Electrochem Soc 129:2016
14. Bouroushian M, Kollia C, Loizos Z, Spyrellis N, Maurin G (1996) Appl Surf Sci 102: 112
15. Loizos Z, Spyrellis N, Maurin G (1991) Thin Solid Films 204: 139
16. Froment M, Bernard MC, Cortes R, Mokili B, Lincot D (1995) J Electrochem Soc 142:2642
17. Cachet H, Cortes R, Froment M, Maurin G, Schramchenko N (1997) In: The Electrochemical Soc. (ed) Proceedings Volume of the Symposium "Electrochemically deposited thin films" San Antonio Vol. 96–19, pp 33–45
18. Stowell MJ (1975) In: Matthews JW (ed) *Epitaxial Growth*, Academic Press, New York, Part B, pp 437–493
19. Sugimoto Y, Peter LM (1995) J Electroanal Chem 381:251
20. Sze SM (1981) Physics of semiconductors devices, 2nd edn. Wiley, New York